RSC Advances

ROYAL SOCIETY OF CHEMISTRY

www.rsc.org/advances

RSC Advances RSC Publishing

ARTICLE

Water-Mediated Promotion of Direct Oxidation of Benzene over Metal-Organic Framework HKUST-1

Cite this: DOI: 10.1039/x0xx00000x

Received 00th January 2014,Accepted 00th January 2014

DOI: 10.1039/x0xx00000x

www.rsc.org/

Yanfeng Liu,[a,b,c] Tianyong Zhang,*[a,b] WubinWu,[a,b] Shuang Jiang,[a,b] Hao Zhang[c] and Bin Li*[a,b]

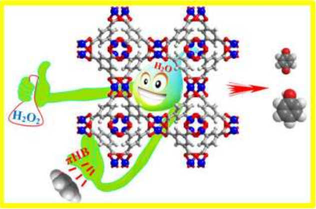

Pretreatment of HKUST-1 catalyst with water significantly accelerated the catalytic oxidation of benzene to phenol and hydroquinone with hydrogen peroxide as oxidant. The corresponding oxygenates had a yield of 36.5 %, and the selectivity to phenol and hydroquinone was 53.2 % and 35.5 %, respectively. The turnover frequency (TOF) was 35.1 h^{-1}. Comparatively, the product yield was only 2.7 % over the original HKUST-1, and the TOF was 2.6 h^{-1}. Moreover, water treatment protected HKUST-1 from decomposition due to formation of a new oxidation mode. Therefore, the catalytic system in the presence of water opened a new door towards a facile and efficient preparation of phenol and hydroquinone.

Introduction

Oxidation of unsaturated C-C bonds in benzene is crucial for synthesis of chemical intermediates in organic chemistry. Nevertheless, it is usually difficult to obtain benzene oxygenates from benzene, because the activating energy of C-H in benzene ring is 111 kcal/mol, higher than those in most alkanes (90-101 kcal/mol) and even higher than that in methane (105 kcal/mol).[1] One-step synthesis of benzene oxygenates with H_2O_2 or molecular oxygen as green oxidants is a great challenge in modern synthetic chemistry.[2] For such purpose, great efforts have been devoted to develop suitable oxidation catalysts. Currently, both homogeneous and heterogeneous catalysts have been extensively investigated, such as Fe^{2+}, Cu^{2+}, Mn^{2+} or V^{2+} complexes, [3] metal-incorporated molecular sieves,[4-5] and carbon-based materials.[6] Among of them, copper-based catalysts have shown a high catalytic activity.[7] Up to now, it has been still attractive to develop a highly efficient and green catalytic route to prepare benzene oxygenates from easily available benzene.

Metal-organic frameworks (MOFs)[8-13] are compounds consisting of metal ions coordinated to organic ligands such as aromatic substances and derivatives,[14] or nitrogen heterocyclic compounds[15] to form one-, two-, or three-dimensional structures. Compared to conventionally used catalysts, MOFs have large surface area,[16] high thermal and chemical stability,[17] as well as diverse skeleton structures obtained by modulating the functional architecture of the metal ions and the organic ligands.[18] Therefore, MOFs have been reported as catalysts or catalyst supports in many catalytic reactions such as oxidation,[19] hydrogenation,[20] Knoevenagel condensation,[21] Suzuki cross-coupling,[22] transesterification reaction,[23] catalytic cracking[24] and aldolcondensation.[25]

According to the reports, copper-based metal-organic framework HKUST-1 has been employed as a heterogeneous catalyst or catalyst support in many reactions such as oxidation, epoxidation, hydroxylation, condensation and esterification.[26] It has a 3D square-shaped porous structure (9 x 9 Å). Commonly, it was also referred to MOF-199 or $[Cu_3(BTC)_2]$, where BTC represents benzene-1,3,5-tricarboxylate. A monomeric unit of the material contains a dicopper cluster with a copper–copper distance of 2.63 Å, in which each copper atom is coordinated by four oxygen atoms from the four BTC linkers, and each BTC binds to three different Cu^{2+} ions.[27] Thus, the coordinative vacancy on Cu^{2+} species occurs naturally in the face-centered crystal lattice of HKUST-1.[28] In this research, original HKUST-1 hardly showed catalytic activity in oxidation of benzene with H_2O_2 as an oxidant in MeCN within 30 minutes. Interestingly, water pretreated HKUST-1 displayed a highly catalytic oxidation activity in the reaction under the same reaction conditions, suggesting that water treatment of this material played an important role in promoting the catalytic activity. Moreover, the absorbed water avoided direct exposure of the active sites on HKUST-1 to H_2O_2 and protected the catalyst from being damaged in the oxidation of benzene. Therefore, the water involved catalytic system opens a green and economical door towards facile oxidation of benzene to its corresponding oxygenates.

Experimental

Materials

Acetonitrile (MeCN, HPLC grade) was acquired from Merck company. The analytical grade solvents of N, N-Dimethylformamide (DMF), ethanol (EtOH), methanol (MeOH), acetone, chlorobenzene and triethylamine were obtained from Sinopharm Chemical Reagent Co. Ltd. Cupric acetate ($Cu(OAc)_2{\cdot}H_2O$) was purchased from Tianjin Damao Chemical Reagent Factory and BTC was purchased from Sun Chemical Technology (Shanghai) Co., Ltd. All materials were used without further purification.

Synthesis of HKUST-1

HKUST-1 was prepared according to a reference.[29] Firstly, a mixture consisting of DMF, EtOH and H_2O was prepared with a volume ratio of 1:1:1. $Cu(OAc)_2{\cdot}H_2O$ (1720 mg, 8.62 mmol) was dissolved in 24 mL of the above mixture solvent under ultrasonic vibration, in which BTC (1000 mg, 4.76 mmol) in 24 mL of the same mixture solvent was dropped with a rate of 0.2 mL/min under vigorous stirring, followed by adding triethylamine (1.0 mL) and stirring at 25 °C for 23 h. The precipitate was separated by vacuum filtration and washed with DMF. Afterwards, the solid was dispersed in 100 mL of CH_2Cl_2 overnight, then separated by vacuum filtration and washed with CH_2Cl_2. The product was dried at 170 °C for 6 h under vacuum.

Characterization

Fourier transform infrared (FTIR) spectra were collected on a Bruker FT-IR Tensor 27 using KBr pellets. Quantification of C, H, and N were performed on an Elementar Vario Micro cube elemental analyzer. Powder X-ray diffraction (XRD) was performed on Rigaku D-Max with 40 kV and Cu-Kα radiation. Thermal gravimetric analyses (TGA) were obtained by a TA Q600 thermal analysis system with ~6 mg of sample in each test. The tests were carried out under a continuous nitrogen flow with a heating rate of 10 °C/min. Surface areas and pore sizes of the samples were assessed via nitrogen physisorption analysis using Quantachrome Autosorb-1. Sample morphologies were observed by scanning electron microscope (SEM) on a Hitachi S4800 with an accelerating voltage 3.0 kV. Raman spectra were collected on a Renishaw in Via Raman Microscope with 514.5 nm laser excitation at room temperature and taken with a 20× microscope objective at 2 mW laser power on the sample. HKUST-1 (7.2 mg) was dispersed in 1 mL of ultra-purified water (an electrical resistance of 18.2 MΩ·cm) for 2 h under ultrasonic of 200 W. Benzene (0.15 mL) was added in the heterogeneous system for a while. The obtained heterogeneous mixture was dropped on the slide for Raman scattering spectrum. Raman spectra were collected from the resulting heterogeneous mixture with an integration time of 2 min for each scattering.

Oxidation of benzene

Firstly, HKUST-1 (140 mg, 0.23 mmol) was immersed in H_2O (20 mL) under ultrasonic of 200 W for different times and separated by centrifugation. All the water treated HKUST-1 samples were denoted as HKUST-1(H_2O)-time. The wet samples were directly used as catalysts for the oxidation of benzene. In a typical reaction, 140 mg of catalyst was placed into a 50 mL two-necked flask with a reflux condenser of ice water. And then, 5 mL of MeCN, 1 mL (11.2 mmol) of benzene and 3mL of H_2O_2 (30 wt %) were added into the flask. The mixture reacted for 0.5 h at 60 °C in a water bath. After the reaction, hydrogen peroxide in the mixture was detected with starch potassium iodide paper. The products were analyzed by a gas chromatograph Agilent 6890 equipped with 30 m of Innowax column and flame ionization detector (FID). Chlorobenzene was used as internal standard.

Results and discussion

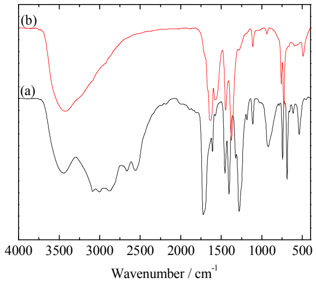

Figure 1 FTIR spectra of samples. (a) BTC, (b) HKUST-1.

The FT-IR spectra of BTC and HKUST-1 were shown in Figure 1. The bands at 1607 and 1454 cm^{-1} in Figure 1a are associated with the C-C skeletal vibration of benzene while the bands at 3086 and 3003 cm^{-1} are attributed to the stretching mode of =C-H in benzene ring. The bands at 1722, 1193, and 919 cm^{-1} are assigned to the C=O stretching, C-O stretching and out-of-plane O-H bending vibration frequencies, respectively, indicating the presence of a carboxylic acid group.[30] The broad band in the region of 3200-2500 cm^{-1} is due to formation of hydrogen bond among the carboxylic acid groups. Compared to BTC (Figure 1a), a significant difference for HKUST-1 (Figure 1b) is that the asymmetric stretch of O=C-O at 1632 cm^{-1} and the symmetric modes at 1374 cm^{-1} can be observed, which confirmed the deprotonation of –COOH groups in BTC upon the reaction with copper metal ions.[30-31] In addition, the band around 760 cm^{-1} is attributed to Cu substituted groups in benzene and the weak band at 1110 cm^{-1} is due to C-O-Cu stretching.[32] The FT-IR analysis of HKUST-1: IR (KBr pellet cm^{-1}) 3444(br), 1632(s), 1582(m), 1444(m), 1374(s), 1110(w), 1060(w), 938(w), 760(m), 729(m), 665(w), 589(w), 489(w), the results are consistent with the literature.[33] It is an indicative of the HKUST-1 structure. In addition, the percentage contents of C, H and N in HKUST-1 were 35.25, 1.29, and 0.02%, respectively. The result fits with Anal. Calcd for HKUST-1 ($[Cu_3(BTC)_2]$): C, 35.64; H, 0.99; N, 0 %.).[33]

XRD patterns of the samples are displayed in Figure 2. The XRD pattern of the as-synthesized HKUST-1 was in good agreement with the simulated one, as shown in Figure 2a and 2b, indicating a high purity of the sample. Figure 2c~2f display the XRD patterns of HKUST-1 samples treated with water for different times. It can be found that the crystalline phase apparently changed due to a possible hydration of HKUST-1. However, among the water treated samples, the diffraction peak

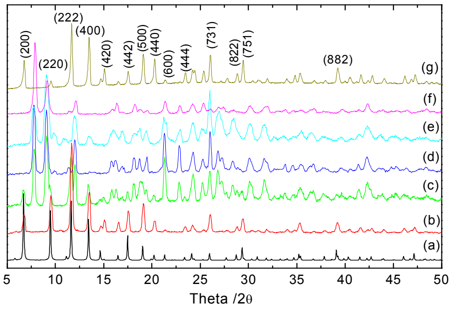

Figure 2 XRD patterns of the samples, (a) simulated from the crystallographic data of HKUST-1 (ref[28]), (b) as-synthesized HKUST-1, (c) HKUST-1(H_2O)-5min, (d) HKUST-1(H_2O)-1h, (e) HKUST-1(H_2O)-2h, (f) HKUST-1(H_2O)-3h, (g) HKUST-1(H_2O) after catalytic reaction.

position and peak numbers of HKUST-1(H_2O)-1h, HKUST-1(H_2O)-2h and HKUST-1(H_2O)-3h were totally similar revealing the same crystalline phase (Figure 2d, 2e and 2f). Surprisingly, the initial crystalline phase of HKUST-1 was recovered after the catalytic oxidation of benzene, despite of slight difference in some peak intensities by comparing Figure 2b to Figure 2g. The intensities of the (200) and (220) crystal planes was changed relatively due to preferred orientation of the crystallites.

The as-synthesized HKUST-1 crystals had a needle-like morphology with a diameter of ~5 nm, as shown in Figure 3a. Comparatively, most of the reported HKUST-1 crystals were octahedral with a size of 15 μm.[34] Besides the crystalline phase, water treatment also changed the morphology evidenced in Figure 3. The HKUST-1(H_2O)-5min looked like rods with a length of over 10 μm (Figure 3b). Nevertheless, the rod-like morphology gradually transformed to tablets, and the crystal size gradually decreased with an increase of the water treatment time (Figure 3c, 3d and 3e). The HKUST-1(H_2O)-1, HKUST-1(H_2O)-2h and HKUST-1(H_2O)-3h were less than 5 μm. The samples were blue as seen from the digital photo in Figure 3f. The appearance of HKUST-1 suspended in water changed gradually with the water treatment time. Figure 3f-2 and 3f-3 showed a relatively homogeneous dispersion of small granules in water. However, the granule size would increase and precipitate due to possible adsorption more water (Figure 3f-4 and 3f-5).

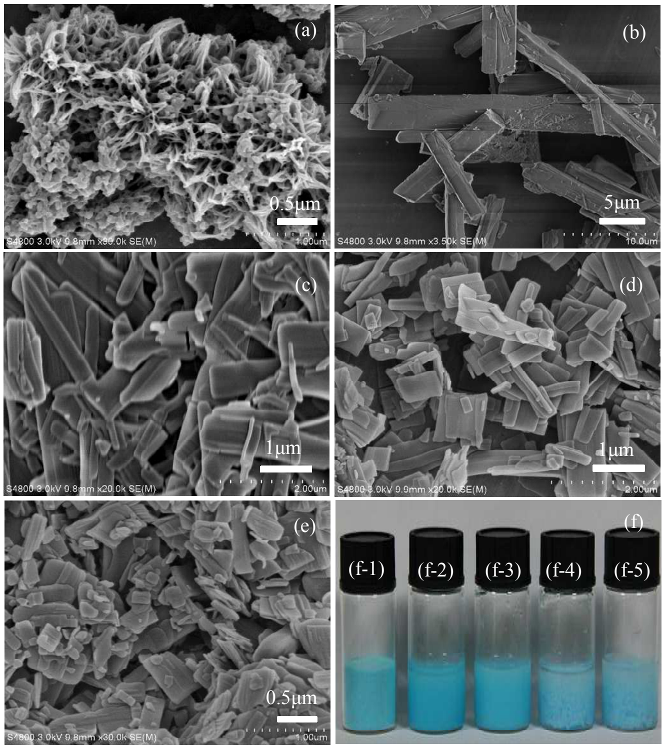

Figure 3 SEM images of HKUST-1 and HKUST-1(H_2O), (a) HKUST-1, (b) HKUST-1(H_2O)-5min, (c) HKUST-1(H_2O)-1h, (d) HKUST-1(H_2O)-2h, (e) HKUST-1(H_2O)-3h, (f) Digital photo of HKUST-1 and HKUST-1(H_2O), (f-1) HKUST-1, (f-2) HKUST-1(H_2O)-5min, (f-3) HKUST-1(H_2O)-1h, (f-4) HKUST-1(H_2O)-2h, (f-5) HKUST-1(H_2O)-3h.

The thermal stabilities of the samples were evaluated by TGA, as shown in Figure 4. The HKUST-1 was dried at 170 °C for 6 h under vacuum for TGA testing. The blue-violet HKUST-1 adsorbed moisture immediately and became deep blue when it was exposed to air. As seen in Figure 4a, the first weight lost stage occurred between 25 °C and 150 °C with a weight loss of 20.0 % for the inevitable air adsorption during TGA analysis. No significant weight loss was seen in the temperature range of 150 °C to 250 °C, indicating the thermal stability of HKUST-1. The second weight loss (48.3 %) started from 250 °C to 420 °C, and the HKUST-1 structure totally collapsed at ~420 °C as reported in literature.[35-36] The process was accompanied by the release of CO_2 due to the decomposition of carboxylic groups and the disintegration of the crystal structure,[37] which led to the formation of Cu_2O and CuO.[35] Before TGA analysis, the wet samples of HKUST-1(H_2O) were exposed to air for around 2 h at ambient temperature to remove free water. Figure 4b revealed two continuous weight loss peaks from 25 °C to 150 °C for the HKUST-1(H_2O)-5min. The weight loss was 27.6 % corresponding to the 13 water molecules per $[Cu_3(BTC)_2(H_2O)_3]$ unit. The theoretical weight loss was 27.9 %.[28] Among them, 3 water molecules complexed with Cu atoms and directed to the interior of nanopores by the terminal axial water ligands, and others were disorder in the accessible pore volume.[28] The similar TGA result was also observed for HKUST-1(H_2O)-1h with a slight enhancement of weight loss by 5.3 %. However, further prolonging the water treatment time, another two continuous weight loss peaks appeared from 120 °C to 250 °C for the HKUST-1(H_2O)-2h and HKUST-1(H_2O)-3h as well as two peaks occurred from 25 °C to 120 °C (Figure 4d and 4e). The weight loss from 120 °C to 250 °C was 5.2 % and 5.1 % for the HKUST-1(H_2O)-2h and HKUST-1(H_2O)-3h, respectively. Figure 4d and 4e were obviously different from Figure 4b and 4c. It implied that some water molecules were possibly absorbed in the relatively small pores. We surmised that HKUST-1(H_2O)-2h and HKUST-1(H_2O)-3h had absorbed water completely, which was also judged from their appearance (Figure 3f-4 and 3f-5).

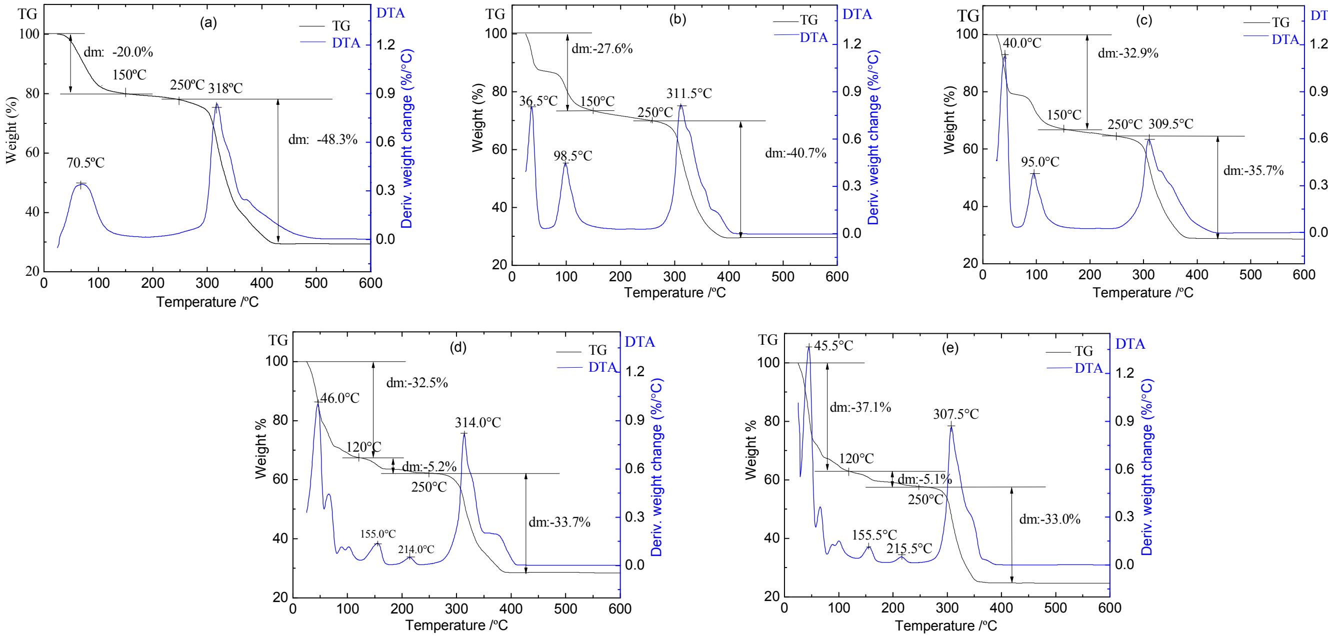

Figure 4 TGA and DTA of the samples. (a) HKUST-1, (b) HKUST-1(H2O)-5min, (c) HKUST-1(H2O)-1h, (d) HKUST-1(H2O)-2h, (e) HKUST-1(H2O)-3h.

The textural properties of HKUST-1 and HKUST-1(H_2O) were summarized in Table 1. After adsorption water, the HKUST-1(H_2O) had much lower BET surface area and pore volume compared to the HKUST-1 due to transformation of the crystal phase caused by water treatment. Figure 4b, 4c, 4d and 4e revealed that the HKUST-1(H_2O) samples had more dense structure and larger size than those of HKUST-1 (Figure 4a). We speculated that relatively small mesopores of HKUST-1(H_2O) disappeared or were wrapped in the interior of solid. The HKUST-1(H_2O) exhibited higher catalytic activities than the HKUST-1 in subsequent oxidation of benzene. Obviously, the adsorpted water on HKUST-1 played a significant role in the catalytic reactions.

Table 1 Surface area and pore volume analysis of HKUST-1(H_2O) and HKUST-1

Entry	Sample	BET surface area (cm^2g^{-1})	Pore volume (cm^3g^{-1})	Pore size (nm)
1	HKUST-1	1095	1.05	173.0
2	HKUST-1(H_2O)-5min	5.67	0.05	26.77
3	HKUST-1(H_2O)-1h	18	0.08	26.78
4	HKUST-1(H_2O)-2h	20.04	0.12	23.98
5	HKUST-1(H_2O)-3h	25	0.14	23.97

Hydroxylation of benzene

In hydroxylation of benzene, MeCN was used as a solvent to disperse the catalyst in the mixture of water and benzene. Without catalyst, the blank run (Table 2, entry 1) did not produce the detectable products. For the original HKUST-1, the product yield was only 2.7 %, and the corresponding TOF was 2.6 h^{-1} at 60 °C (Table 2, entry 2). In the catalytic reaction, the color of the mixture changed slightly, indirectly suggesting a very slow oxidation of benzene. Comparatively, when HKUST-1(H_2O)-2h, water treated HKUST-1, was applied to the oxidation of benzene, the reaction mixtures changed into dark green in the first 4 min, then changed into brown immediately in 6-8 min, and then kept brown in the reaction, which revealed that the reaction proceeded very fast. The product yield was increased to 36.5 %, the TOF was 35.1 h^{-1}, and the selectivity of phenol was 53.2 % (Table 2, entry 3). The effect of reaction temperature was also investigated over the HKUST-1(H_2O)-2h. The yields were low as the temperature below 60 °C (Table 2, entry 4-6). Meanwhile, it can be found that the yield was rapidly decreased to 13.8 % at 70 °C due to the rapid decomposition of H_2O_2, because we observed that a large number of bubbles violently generated in the reaction at 70 °C. After each reaction,

Table 2 Catalytic performance of HKUST-1 and HKUST-1(H_2O) in the oxidation of benzene.

Entry	Catalyst	Selectivity of the oxygenates (%)				Yield (%)	TOF (h^{-1})
		PH	BE	CA	HY		
1	None	0	0	0	0	0	0
2	HKUST-1	36.0	61.9	0	2.1	2.7	2.6
3	HKUST-1(H_2O)[a]	53.2	1.5	9.8	35.5	36.5	35.1
4	HKUST-1(H_2O)[b]	43.1	43.1	2.4	11.4	12.6	13.5
5	HKUST-1(H2O)[c]	52.0	5.3	16.4	26.3	18.2	19.5
6	HKUST-1(H_2O)[d]	56.9	2.8	14.2	26.1	13.8	14.8
7	HKUST-1(H_2O)-5min	41.5	38.7	0	19.8	7.5	7.4
8	HKUST-1(H_2O)-1h	77.0	5.2	0	17.8	9.5	9.3
9	HKUST-1(H_2O)-3h	53.1	2.3	7.8	36.8	35.8	34.9
10	HKUST-1(Dehydration)	54.4	43.8	0	1.8	6.6	6.4

PH=phenol, BE=benzoquinone, CA=catechol, HY=hydroquinone;
[a, b, c, d] The temperature of the water bath was 60 °C, 40 °C, 50 °C and 70 °C respectively.
TOF = mole of the oxygenates / (mole of HKUST-1 × reaction time)
Selectivity = mole of some oxygenate / mole of all the oxygenates
Yield = mole of all the oxygenates / mole of benzene

starch potassium iodide paper was used to detect H_2O_2 left in the reaction mixture. However, no color change was observed on the starch potassium iodide paper, which meant that H_2O_2 was exhausted. Therefore, the optimum reaction temperature was ~ 60 °C.

The catalytic performance of HKUST-1(H_2O) might be affected by the adsorption level of water. Inspired by this idea, the wet samples of HKUST-1(H_2O) with different water treating times were tested in the oxidation of benzene. Since the HKUST-1(H_2O)-2h and HKUST-1(H_2O)-3h had sufficiently adsorbed water (Figure 4d, 4e), their catalytic activities were much higher than those of HKUST-1(H_2O)-5min and HKUST-1(H_2O)-1h (Table 2, entry 4, 7, 8 and 9). In other words, the water in the small pores as well as that in the big pores or on the surface of HKUST-1 played significant roles in enhancing the catalytic activity.

Meanwhile, ultrasonic treatment broke the HKUST-1 crystals and might increase the outside surface area, which was confirmed by some relative works. However, ultrasonic disruption was not the key factor for the enhancement of catalytic activities. When the wet broken HKUST-1(H_2O)-2h was dewatered at 100 °C for 3 h under vacuum, the product yield was decreased to 6.6 % from 36.5 % for the wet HKUST-1(H_2O)-2h (Table 2, entry 3, 10). Hence, water played more significant role in the promotion of catalytic activity than the crystal size.

To further confirm that water promoted the reactivity of HKUST-1 in the hydroxylation of benzene, HKUST-1 (140 mg, 0.23 mmol) was treated with other solvents (DMF, EtOH, MeOH, MeCN and acetone) for 2 h. The obtained samples were named as HKUST-1(solvent), where the solvent in the bracket referred to DMF, EtOH, MeOH, MeCN and acetone. Then the HKUST-1(solvent) was also applied to the oxidation of benzene under the investigated conditions. However, these solvents treated HKUST-1 didn't significantly improve the yield compared with the HKUST-1, as shown in Table 3.

Table 3 Catalytic activity of the HKUST-1 pretreated by different solvents in the oxidation of benzene

Entry	Catalyst	Selectivity of the oxygenates (%)				Yield (%)	TOF (h^{-1})
		PH	BE	CA	HY		
1	HKUST-1(H_2O)	53.2	1.5	9.8	35.5	36.5	35.1
2	HKUST-1(DMF)	79.8	20.2	0	0	1.2	1.1
3	HKUST-1(EtOH)	60.8	39.2	0	0	1.9	1.9
4	HKUST-1(MeOH)	63.0	37.0	0	0	1.3	1.2
5	HKUST-1(MeCN)	52.6	47.4	0	0	4.8	4.6
6	HKUST-1(Acetone)	61.1	38.9	0	0	0.5	0.5

Catalytic reaction conditions: 140 mg of HKUST-1(solvent), 5 mL of MeCN , 1mL of benzene (11.2 mmol) and 3 mL of 30 (wt)% H_2O_2 (29.4 mmol) were mixed and heated in a water bath at 60 °C for 0.5 h.

To study of the catalysts reusability, the HKUST-1(H_2O)-2h and the HKUST-1 were reused three times in the oxidation of benzene under investigated conditions. The catalysts were washed with 3×5 mL of H_2O after each reaction and reused. The results were listed in Table 4. It indicated that the catalyst HKUST-1(H_2O)-2h could be reused for more than twice without mainly loss of activity. And for HKUST-1, when it was employed a second time in the reaction, a slight improvement in activity was observed. This enhancement in activity could probably be considered that the water contributed a lot in the activity of the catalyst HKUST-1 (Table 4).

Table 4 Reusability of the HKUST-1(H_2O) and HKUST-1 in the oxidation of benzene [a]

Recycle time	catalysts	Selectivity of the oxygenates (%)				Yield (%)	TOF (h^{-1})
		PH	BE	CA	HY		
1	HKUST-1(H_2O)-2h	53.2	1.5	9.8	35.5	36.5	35.1
2		46.9	41.7	4.0	7.4	35.2	33.8
3		41.1	36.8	10.2	11.9	11.9	11.4
1	HKUST-1	36.0	61.9	0	2.1	2.7	2.6
2		43.1	47.6	0.0	9.3	4.8	4.6
3		45.6	50.1	0.0	4.3	2.1	2.0

[a] Conditions: 140 mg of catalyst, 5 mL of MeCN, 1mL of benzene (11.2 mmol) and 3 mL of 30 (wt)% H_2O_2, 60 °C, 0.5 h.

Catalytic mechanism of HKUST-1(H_2O)

To identify the catalytic sites on the HKUST-1 in the oxidation of benzene, we examined the catalytic efficiency of BTC in the reaction. The reaction did not proceed when the same amount of BTC was employed as a substitute for HKUST-1, suggesting that the constituent metal ions (i.e. Cu^{2+}) in the HKUST-1 structure were the catalytic sites. The unsaturated copper can be hydrated in water for several minutes and dehydrated under vacuum. The crystalline phase of HKUST-1 was changed upon adsorpting water (Figure 2c, 2d, 2e and 2f). However, the original crystalline phase can be recovered after being used as catalyst for twice (Figure 2g), which indicated that the crystalline structure of HKUST-1 maintained stable in water for a certain period of time. HKUST-1 shows high structural stability upon water adsorption or desorption.[38]

The catalytic characteristics of HKUST-1 are determined not only by the coordinative position of Cu^{2+} available for bonding small molecules, but also by the dispersive interactions of the organic ligand of BTC. HKUST-1 possesses an intersecting 3D channels with large square-shaped pores (9 Å by 9 Å)[28, 39] and Lewis acid coordination sites (open copper sites) on the interior walls of the pores.[40] In addition, HKUST-1 consists of two types of "cages", which was separated by two types of "windows".[33, 41] Such crystal structure and pore feature facilitate absorption of water. The pores contain 3 terminal axial water molecules whose ligands are directed from the Cu atoms to the interior of the nanopores and up to 10 additional water molecules per $[Cu_3(BTC)_2(H_2O)_3]_n$ unit by thermal gravimetric analysis (TGA) (Figure 4), as is in accord with the literature.[28] When HKUST-1 was used as catalyst, π-π interaction of the aromatic rings of benzene with the BTC framework and π-complexation of electron-rich benzene to the Lewis acid sites in HKUST-1[40, 42] were not propitious to the interaction of benzene with Cu^{2+} active sites in HKUST-1. However, interestingly, the utilization of catalyst, the reaction rate and the yield of oxygenates were improved significantly for the same reaction with HKUST-1(H_2O) as catalyst. Actually, in aqueous solution containing benzene, water-water hydrogen bond (wHB) provides an energetically and statistically competitive alternative to benzene-water π H-bond (πHB).[43] H atom of H_2O points toward the π-cloud of benzene to form O-H···π H-bond, and H_2O interacts with the benzene via O-H···π H-bond.[44] It is a formidable challenge to obtain the evidence of the πHB formation between benzene and water because of the low aqueous solubility of benzene (~20 mM), which means that the πHB OH vibrational peak of interest is more than 1000 times smaller than the broad overlying bulk water OH stretch band. The Raman spectrum of HKUST-1, H_2O and benzene revealed a small, broad OH peak at ~3610 cm^{-1} assigned to a πHB peak between benzene and H_2O,[43] as shown in Figure 5. High-resolution rotational and in vibrational spectra of πHB benzene-H_2O dimer indicate that the formation of a πHB leaves water remarkable free to rotate,[45] which reveals that πHB is far more flexible (has greater entropy) than OH···O hydrogen bonds.[43] The water molecule nearest to benzene's center of mass has a greater conformational flexibility when one of its two OH groups forms a πHB than it does when both of its OH groups form a wHB.[43] The water molecules existing in the pores of the HKUST-1 or surrounding around the HKUST-1 interacting with benzene via πHB ought to impel benzene to contact with the Cu^{2+} sites.

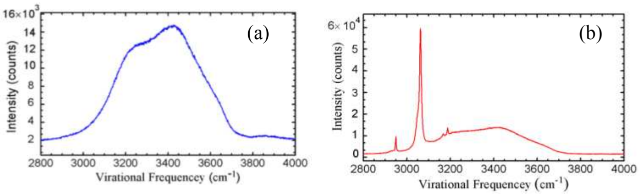

Figure 5 Aqueous solutions containing dissolved benzene reveal vibrational peaks assigned to water πHB OH groups. (a) The total Raman scattering spectrum of HKUST-1 in water looks virtually identical to that of bulk water. (b) The resulting Raman spectrum of HKUST-1, water and benzene reveals a small, relatively broad peak at ~3610 cm^{-1} assigned to a πHB peak between benzene and liquid water.

Scheme 1 Proposed reaction pathway for the oxidation of benzene on the initial HKUST-1 and water-mediated HKUST-1

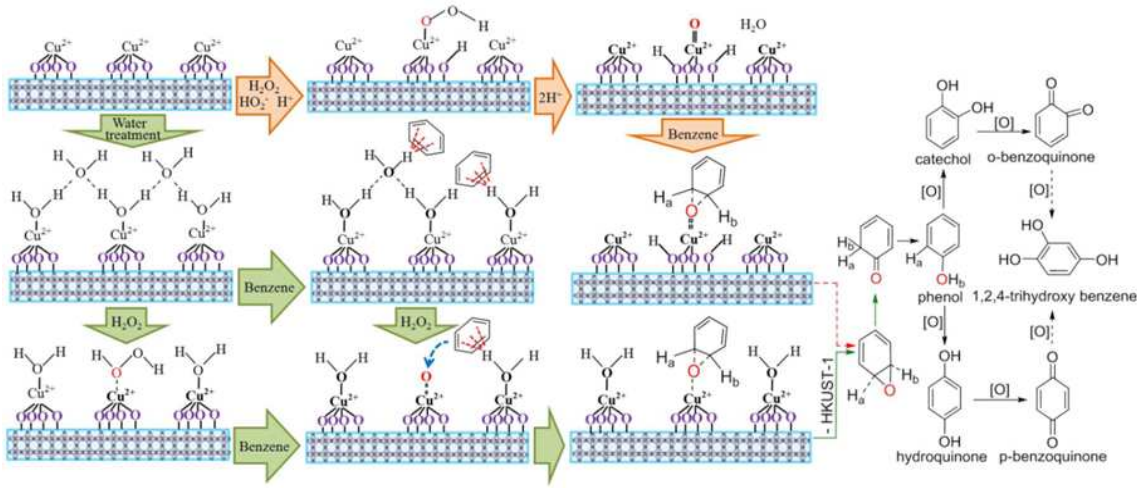

Considering all the above results, we propose a comprehensive summary of the mechanisms of the catalytic process of benzene on both HKUST-1 and HKUST-1(H_2O), as schematized in Scheme 1. In the case of using the HKUST-1 as the catalyst, owing to the adsorption of H_2O_2 on HKUST-1, it was very likely the negative HO_2^- ions dissociated from H_2O_2 directly coordinate to the copper sites to form –Cu=O,[46] and then benzene bonds to O atom of –Cu=O by the intermolecular bonds to produce phenol. However, in this process, –Cu=O is formed and simultaneously two sites of coordination between Cu and BTC are lost, the previously coordinated BTC units have to be released, that is, the coordination sites between Cu and BTC would reduce. However, interestingly, the yield of oxygenates, reaction speed, and the stability of HKUST-1 underwent pronounced improvement using HKUST-1(H_2O) as catalyst for the oxidation of benzene. The water-mediated promotion of catalytic activity of HKUST-1 is described in Scheme 1. Water can be coordinated to the Cu sites by strong metal-organic bond, and simultaneously additional water molecules can retain in the pores of HKUST-1 and surroundings around HKUST-1 through hydrogen-bonding interactions or physical adsorption. Water bonding and solvation of surrounding bulk water are the keys for the switch of benzene adsorption mode, the promotion of catalyst reactivity and the enhancement of products yield. We speculated that H_2O_2 can coordinate to Cu sites instantaneously by situ substitution for water, which can be highly effective in protecting the structure of HKUST-1. In addition, benzene interacting with water molecules coordinated to Cu sites or retained in pores or surroundings of HKUST-1 via O-H···π H-bond has been certified by analysis of Raman scattering spectrum, which spurs benzene approach the active sites of HKUST-1 and accelerates the reaction of benzene with H_2O_2. With this consideration, the effect should be valid for the oxidation of single ring aromatic substances with H_2O_2 as oxidant.

Conclusions

In summary, we have disclosed a novel catalytic system in the presence of HKUST-1 preadsorbed water for the oxidation of benzene with H_2O_2 as oxidant. Simple water treatment can significantly rearrange reaction mode of H_2O_2 with HKUST-1, switch adsorption mode of benzene, promote catalyst reactivity and enhance products yield. The catalytic system with water active participation opens a door toward facile improvement in the reaction efficiency of the direct oxidation of benzene to its corresponding oxygenates with a simple, green, and cheap method. In addition, the present work reminds us of some important but often ignored issues. Furthermore, the combination of water with HKUST-1 is expected to be utilized in the oxidation of other single ring aromatic substances with H_2O_2.

Acknowledgements

Funding supports from National Natural Science Foundation of China (21103121, 21276187), Research Fund for the Doctoral Program of Higher Education of China (20110032120011), and Tianjin Municipal Natural Science Foundation (13JCQNJC05800) are gratefully acknowledged.

Notes and references

[a]School of Chemical Engineering and Technology, Tianjin University, Tianjin 300072, China. E-mail: tyzhang@tju.edu.cn, libin@tju.edu.cn
[b]Collaborative Innovation Center of Chemical Science and Engineering (Tianjin), Tianjin 300072, China
[c]School of Material and Chemical Engineering, Hainan University, Haikou 570228, China

1 J. M. Mayer, In Biomimetic Oxidations Catalyzed by Transition Metal Complexes. London: Imperial College Press, 2000.
2 S. -I. Niwa, M. Eswaramoorthy, J. Nair, A. Raj, N. Itoh, H. Shoji, T. Namba and F. Mizukami, Science, 2002, 295, 105.
3 (a) A. Raba, M. Cokoja, W. A. Herrmann and F. E. Kühn, Chem. Commun., 2014, 50, 11454; (b) L. M. Zhao, Z. C. Liu, W. Y. Guo, L. Z. Zhang, F. Y. Zhang, H. Y. Zhu and H. H. Shan, Phys. Chem. Chem. Phys., 2009, 11, 4219; (c) H. Yang, Q. Wu, J. Li, W. Dai, H. Y. Zhang, D. Lu, S. Gao and W. S. You, Appl. Catal. A: Gen., 2013, 457, 21; (d) X. Wang, T. Zhang, Q. Yang, S. Jiang and B. Li, Eur. J. Inorg. Chem., 2015, 5, 817; (e) Y. Wang, T. Zhang, B. Li, S. Jiang and L. Sheng, RSC Advances, 2015, 5, 29022.
4 A. B. Ene, T. Archipov and E. Roduner, J. Phys. Chem. C, 2011, 115, 3688.
5 L. Hu, B. Yue, X. Chen and H. He, Catal. Commun., 2014, 43, 179.
6 W. Wang, G. Ding, T. Jiang, P. Zhang, T. Wu and B. Han, Green Chem., 2013, 15, 1150.
7 P. Nagababu, S. Maji, M. P. Kumar, P. P. -Y. Chen, S. S. -F. Yu and S. I. Chan, Adv. Synth. Catal., 2012, 354, 3275.
8 B. D. Chandler, J. O. Yu, D. T. Cramb and G. K. H. Shimizu, Chem. Mater., 2007, 19, 4467.
9 G. Chaplais, A. Simon-Masseron, F. Porcher, C. Lecomte, D. Bazer-Bachi, N. Bats and J. Patarin, Phys. Chem. Chem. Phys., 2009, 11, 5241.
10 P. Jain, V. Ramachandran, R. J. Clark, H. D. Zhou, B. H. Toby, N. S. Dalal, H. W. Kroto and A. K. Cheetham, J. Am. Chem. Soc., 2009, 131, 13625.
11 B. Cai, P. Yang, J. W. Dai and J. Z. Wu, Cryst. Eng. Commun., 2011, 13, 985.
12 D. X. Xue, A. J. Cairns, Y. Belmabkhout, L. Wojtas, Y. Liu, M. H. Alkordi and M. Eddaoudi, J. Am. Chem. Soc., 2013, 135, 7660.
13 H, Furukawa, K. E. Cordova, M. O'Keeffe and O. M. Yaghi, Science, 2013, 341, 974.
14 J. Kim, D. O. Kim, D. W. Kim and K. Sagong, J. Solid State Chem., 2013, 197, 261.
15 (a) H. L. Gao, L. Yi, B. Zhao, X. Q. Zhao, P. Cheng, D. Z. Liao and S. P. Yan, Inorg. Chem., 2006, 45, 5980; (b) J. An, S. J. Geib and N. L. Rosi, J. Am. Chem. Soc., 2009, 132, 38; (c) W. L. Liu, L. H. Ye, X. F. Liu, L. M. Yuan, X. L. Lu and J. X. Jiang, Inorg. Chem. Commun., 2008, 11, 1250; (d) W. Morris, B. Volosskiy, S. Demir, F. Gándara, P. L. McGrier, H. Furukawa, D. Cascio, J. F. Stoddart and O. M. Yaghi, Inorg. Chem., 2012, 51, 6443.
16 (a) K. Sumida, D. L. Rogow, J. A. Mason, T. M. McDonald, E. D. Bloch, Z. R. Herm, T. -H. Bae and J. R. Long, Chem. Rev., 2012, 112, 724; (b) J. -R. Li, J. Sculley and H. -C. Zhou, Chem. Rev., 2012, 112, 869; (c) O. K. Farha, I. Eryazici, N. C. Jeong, B. G. Hauser, C. E. Wilmer, A. A. Sarjeant, R. Q. Snurr, S. T. Nguyen, A. Ö. Yazaydin and J. T. Hupp, J. Am. Chem. Soc., 2012, 134, 15016; (d) J. A. Mason, M. Veenstra and J. R. Long, Chem. Sci., 2014, 5, 32.
17 (a) V. Colombo, S. Galli, H. J. Choi, G. D. Han, A. Maspero, G. Palmisano, N. Masciocchi and J. R. Long, Chem. Sci., 2011, 2, 1311; (b) I. J. Kang, N. A. Khan, E. Haque and S. H. Jhung, Chem. Eur. J. 2011, 17, 6437; (c) T. Li, F. L. Wang, S. T. Wu, X. H. Huang, S. M. Chen and C. C. Huang, Cryst. Growth Des., 2013, 13, 271.
18 (a) H. D. Guo, X. M. Guo, H. Y. Zou, Y. J. Qi and R. Z. Chen, Cryst. Eng. Commun., 2014, 16, 2176; (b) V. Guillerm, D. Kim, J. F. Eubank, R. Luebke, X. F. Liu, K. Adil, M. S. Lah and M. Eddaoudi, Chem. Soc. Rev., 2014, 43, 6141; (c) A. Schneemann, V. Bon, I. Schwedler, I. Senkovska, S. Kaskel and R. A. Fischer, Chem. Soc. Rev., 2014, 43, 6062.
19 J. L. Long, L. M. Wang, X. F. Gao, C. H. Bai, H. F. Jiang and Y. W. Li, Chem. Comm., 2012, 48, 12109.
20 S. Schuster, E. Klemm and M. Bauer, Chem. –Eur. J., 2012, 19, 15831.
21 Y. K. Hwang, D. Y. Hong, J. S. Chang, H. Seo, M. Yoon, J. Kim, S. H. Jhung, C. Serre, and G. Férey, Appl. Catal. A: Gen., 2009, 358, 249.
22 V. Pascanu, Q. X. Yao, A. B. Gómez, M. Gustafsson, Y. F. Yun, W. Wan, L. Samain, X. D. Zou and B. Martín-Matute, Chem. –Eur. J., 2013, 19, 17483.
23 C. Chizallet, S. Lazare, D. Bazer-Bachi, F. Bonnier, V. Lecocq, E. Soyer, A. -A. Quoineaud and N. Bats, J. Am. Chem. Soc., 2010, 132, 12365.
24 A. Corma, M. J. Diaz-Cabanas, J. L. Jorda, C. Martinez and M. Moline, Nature, 2006, 443, 842.
25 S. Horike, M. Dincă, K. Tamaki and J. R. Long, J. Am. Chem. Soc., 2008, 130, 5854.
26 (a) J. M. Zamaro, N. C. Pérez, E. E. Miró, C. Casado, B. Seoane, C. Téllez and J. Coronas, Chem. Eng. J., 2012, 195-196, 180; (b) S. Abednatanzi, A. Abbasi and M. Masteri-Farahani, J. Mol. Catal. A-Chem., 2015, 399, 10; (c) H. Yang, J. Li, H. Zhang, Y. Lv and S. Gao, Micropor. Mesopor. Mater., 2014, 195, 87; (d) Q. Luo, X. Song, M. Ji, S. Park, C. Hao and Y. Li, Appl. Catal. A: Gen., 2014, 478, 81; (e) S. A. Sotnik, K. S. Gavrilenko, A. S. Lytvynenko and S. V. Kolotilov, Inorg. Chim. Acta, 2015, 426, 119; (f) L. H. Wee, N. Janssens, S. R. Bajpe, C. E. A. Kirschhock and J. A. Martens, Catal. Today, 2011, 171, 275.
27 L. Alaerts, E. Séguin, H. Poelman, F. Thibault-Starzyk, P. A. Jacobs and D. E. DeVos, Chem. Eur. J., 2006, 127, 353.
28 S. S. Y. Chui, S. M. F. Lo, J. P. H. Charmant, A. G. Orpen and I. D. Williams, Science, 1999, 283, 1148.
29 D. J. Tranchemontagne, J. R. Hunt and O. M. Yaghi, Tetrahedron, 2008, 64, 8553.
30 L. T. L. Nguyen, T. T. Nguyen, K. D. Nguyen and N. T. S. Phan, Appl. Catal. A: Gen., 2012, 425-426, 44.
31 C. H. Specht and F. H. Frimmel, Phys. Chem. Chem. Phys., 2011, 3, 5444.
32 J. Hu, H. Cai, H. Ren, Y. Wei, Z. Xu, H. Liu and Y. Hu, Ind. Eng. Chem. Res., 2010, 49, 12605.
33 J. L. C. Rowsell and O. M. Yaghi, J. Am. Chem. Soc., 2006, 128, 1304.
34 K. S. Lin, A. K. Adhikari, C. N. Ku, C. L. Chiang and H. Kuo, Int. J. Hydrogen Energy, 2012, 37, 13865.
35 Y. K. Seo, G. Hundal, I. T. Jang, Y. K. Hwang, C. H. Jun and J. S. Chang, Micropor. Mesopor. Mater., 2009, 119, 331.

36 Q. M. Wang, D. Shen, M. Bülow, M. L. Lau, S. Deng, F. R. Fitch, N. O. Lemcoff and J. Semanscin, Micropor. Mesopor. Mater., 2002, 55, 217.

37 G. S. Szymanski, Z. Karpinski, S. Biniak and A. Swatkowski, Carbon, 2002, 40, 2627.

38 K. Schlichet, T. Kratzke and S. Kaskel, Micropor. Mesopor. Mater., 2004, 73, 81.

39 A. Vishnyakow, P. I. Ravikovitch, A. V. Neimark, M. Bülow and Q. M. Wang, Nano Lett., 2003, 3, 713.

40 X. Y. Cui, Z. Y. Gu, D. Q. Jiang, Y. Li, H. F. Wang and X. P. Yan, Anal. Chem., 2009, 81, 9771.

41 C. Chmelic, J. Kärger, M. Wiebcke, J. Caro, J. M. van Baten and R. Krishna, Micropor. Mesopor. Mater., 2008, 117, 22.

42 Z. Y. Gu, C. X. Yang, N. Chang and X. P. Yan, Acc. Chem. Res., 2012, 45, 734.

43 K. P. Gierszal, J. G. Davis, M. D. Hands, D. S. Wilcox, L. V. Slipchenko and D. Ben-Amotz, J. Phys. Chem. Lett., 2011, 2, 2930.

44 M. Prakash, K. G. Samy and V. Subramanian, J. Phys. Chem. A, 2009, 113, 13845.

45 (a) S. Suzuki, P.G. Green, R. E. Bumgarner, S. Dasgupta, W. A. Goddard and G. A. Blake, Science, 1992, 257, 924; (b) R. N. Pribble, A. W. Garrett, K. Haber and T. S. Zwier, J. Chem. Phys., 1995, 103, 531; (C) J. Gruenloh, J. R. Carney, C. A. Arrington, T. S. Zwier, S. Y. Fredericks and K. D. Jordan, Science, 1997, 276, 1678; (d) J. Gruenloh, J. R. Carney, F. C. Hagemeister, T. S. Zwier, J. T. Wood and K. D. Jordan, J. Chem. Phys., 2000, 113, 2290.

46 C. Petit, B. Levasseur, B. Mendoza and T. J. Bandosz, Micropor. Mesopor. Mater., 2012, 154, 107.